Radiation Report

LMP7704-SP SEE Report

ABSTRACT

This study characterizes the various Single-Event Effects (SEE) of heavy-ion irradiation of the LMP7704-SP. This device is a radiation-hardened, quad-channel, low offset voltage, rail-to-rail input and output (RRIO) precision amplifier with a CMOS input stage. No incidences of Single-Event Latch-up (SEL) were detected up to LET_{EFF} = 85 MeV-cm^2/mg at 125°C. Single-Event Transients (SET) were detected and characterized from LET_{EFF} 2 to 85 MeV-cm^2/mg at 25°C.

Table of Contents

List of Figures

List of Tables

Trademarks

All trademarks are the property of their respective owners.

1 Overview

The LMP7704-SP is a precision amplifier with low input bias, low offset voltage, 2.5-MHz gain bandwidth product, and a wide supply voltage. The device is radiation hardened and operates in the military temperature range of −55°C to +125°C.

The high dc precision of this amplifier, specifically the low offset voltage of ±60 µV and ultra-low input bias of ±500 fA, make this device an excellent choice for interfacing with precision sensors with high-output impedances. This amplifier can be configured for transducer, bridge, strain gauge, and transimpedance amplification.

Table 1-1. Overview Information[1]

DESCRIPTION	DEVICE INFORMATION
TI Part Number	LMP7704-SP
MLS Number	5962-1920601VXC
Device Function	Radiation Hardness Assured (RHA), Precision, Low Input Bias, RRIO, Wide Supply Range Amplifiers
Technology	VIP050
Exposure Facility	Radiation Effects Facility, Cyclotron Institute, Texas A&M University
Heavy Ion Fluence per Run	1×10^6 – 1×10^7 ions/cm^2
Irradiation Temperature	125°C (for SEL testing)

(1) TI may provide technical, applications or design advice, quality characterization, and reliability data or service, providing these items shall not expand or otherwise affect TI's warranties as set forth in the Texas Instruments Incorporated Standard Terms and Conditions of Sale for Semiconductor Products and no obligation or liability shall arise from Semiconductor Products and no obligation or liability shall arise from TI's provision of such items.

2 SEE Mechanisms

The primary single-event effect (SEE) events of interest in the LMP7704-SP are single-event latch-up (SEL). From a risk and impact point-of-view, the occurrence of an SEL is potentially the most destructive SEE event and the biggest concern for space applications. The VIP050 process was used for the LMP7704-SP. CMOS circuitry introduces a potential for SEL susceptibility. SEL can occur if excess current injection caused by the passage of an energetic ion is high enough to trigger the formation of a parasitic cross-coupled PNP and NPN bipolar structure (formed between the p-sub and n-well and n+ and p+ contacts). The parasitic bipolar structure initiated by a single-event creates a high-conductance path (inducing a steady-state current that is typically orders-of-magnitude higher than the normal operating current) between power and ground that persists (is *latched*) until power is removed or until the device is destroyed by the high-current state.

This study was performed to evaluate the SEL effects with a bias voltage of 5.5 V on V_{IN} and supply voltage of 12 V (V_S = ±6 V). Heavy ions with LET_{EFF} = 85 MeV-cm^2/mg were used to irradiate the devices. Flux of 10^5 ions/s-cm^2 and fluence of 10^7 ions/cm^2 were used during the exposure at 125°C. The VIP050 process modifications applied for SEL mitigation were shown to be sufficient because the LMP7704-SP exhibited no SEL with heavy-ions up to an LET_{EFF} of 85 MeV-cm^2/mg at a fluence of 10^7 ions/cm^2 and a chip temperature of 125°C.

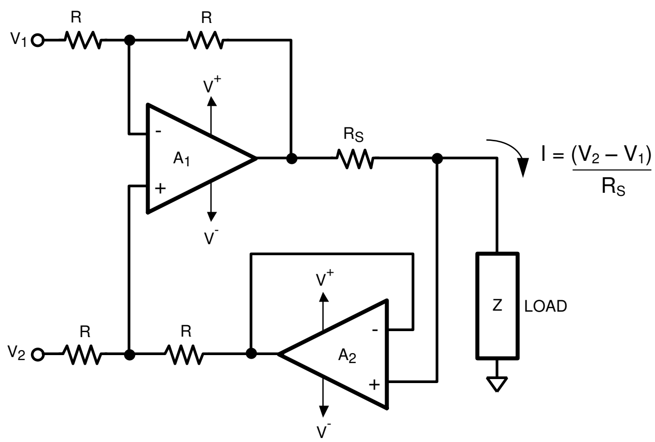

Figure 2-1. Typical LMP7704-SP Application Diagram

3 Test Device and Test Board Information

The LMP7704-SP is packaged in an 14-pin, HBH CFP shown with pinout in Figure 3-1. Figure 3-2 shows the LMP7704-SP bias diagram.

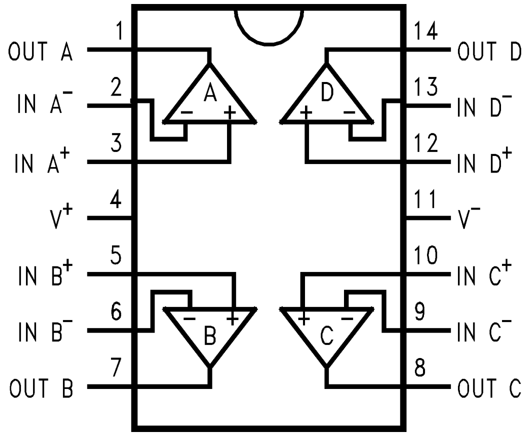

Figure 3-1. LMP7704-SP Pinout

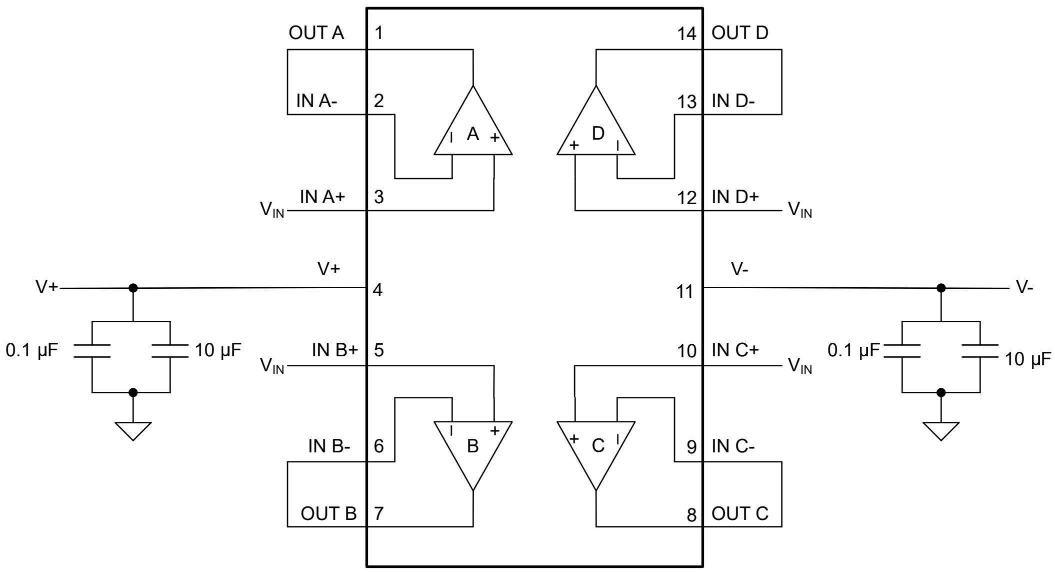

Figure 3-2. LMP7704-SP Bias Diagram

4 Irradiation Facility and Setup

The heavy ion species used for the SEE studies on this product were provided and delivered by the TAMU Cyclotron Radiation Effects Facility[3] using a superconducting cyclotron and advanced electron cyclotron resonance (ECR) ion source. Ion beams are delivered with high uniformity over a 1-inch diameter circular cross sectional area for the in-air station. Uniformity is achieved by means of magnetic defocusing. The intensity of the beam is regulated over a broad range spanning several orders of magnitude. For the bulk of these studies, ion fluxes between 10^4 and 10^5 ions/s-cm^2 were used to provide heavy ion fluences between 10^6 and 10^7 ions/cm^2. For these experiments Praseodymium (Pr) ions were used. Ion beam uniformity for all tests was in the range of 91% to 98%.

5 SEL Results

During SEL characterization, the device was heated using forced hot air, maintaining the IC temperature at 125°C. The temperature was monitored by means of a K-type thermocouple attached as close to the IC as possible. The species used for the SEL testing was a Praseodymium (^{59}Pr) ion with an angle-of-incidence of 39° for an LET_{EFF} = 85 MeV-cm^2/mg. The kinetic energy in the vacuum for this ion is 2.114 GeV (15-MeV/amu line). A flux of approximately 10^5 ions/s-cm^2 and a fluence of approximately 10^7 ions/cm^2 were used for two runs. The V_S supply voltage is supplied externally onboard at the recommended maximum voltage setting of 12 V. Run duration to achieve this fluence was approximately 2 minutes. No SEL events were observed during both runs shown in Table 5-1. Figure 5-1 shows a plot of the current vs time.

Table 5-1. LMP7704-SP SEL Conditions Using ^{59}Pr at an Angle-of-Incidence of 39°

RUN #	DISTANCE (mm)	TEMPERATURE (°C)	ION	ANGLE	FLUX (ions/s-cm^2)	FLUENCE (ions/cm^2)	LET_{EFF} (MeV-cm^2/mg)
10	40	125	Pr	39°	1.00E+05	1.00E+07	85
311	40	125	Pr	39°	1.00E+05	1.00E+07	85

No SEL events were observed, indicating that the LMP7704-SP is SEL-immune at LET_{EFF} = 85 MeV-cm^2/mg and T = 125°C. Using the MFTF method described in Appendix A and combining (or summing) the fluences of the two runs at 125°C (2 × 10^7 ions/cm^2), the upper-bound cross-section (using a 95% confidence level) is calculated in Equation 1:

$$\sigma SEL \leq 1.84 \times 10^{-7}\ \text{cm}^2 \text{ for } LET_{EFF} = 85\ \text{MeV-cm}^2\text{/mg and } T = 125°C \quad (1)$$

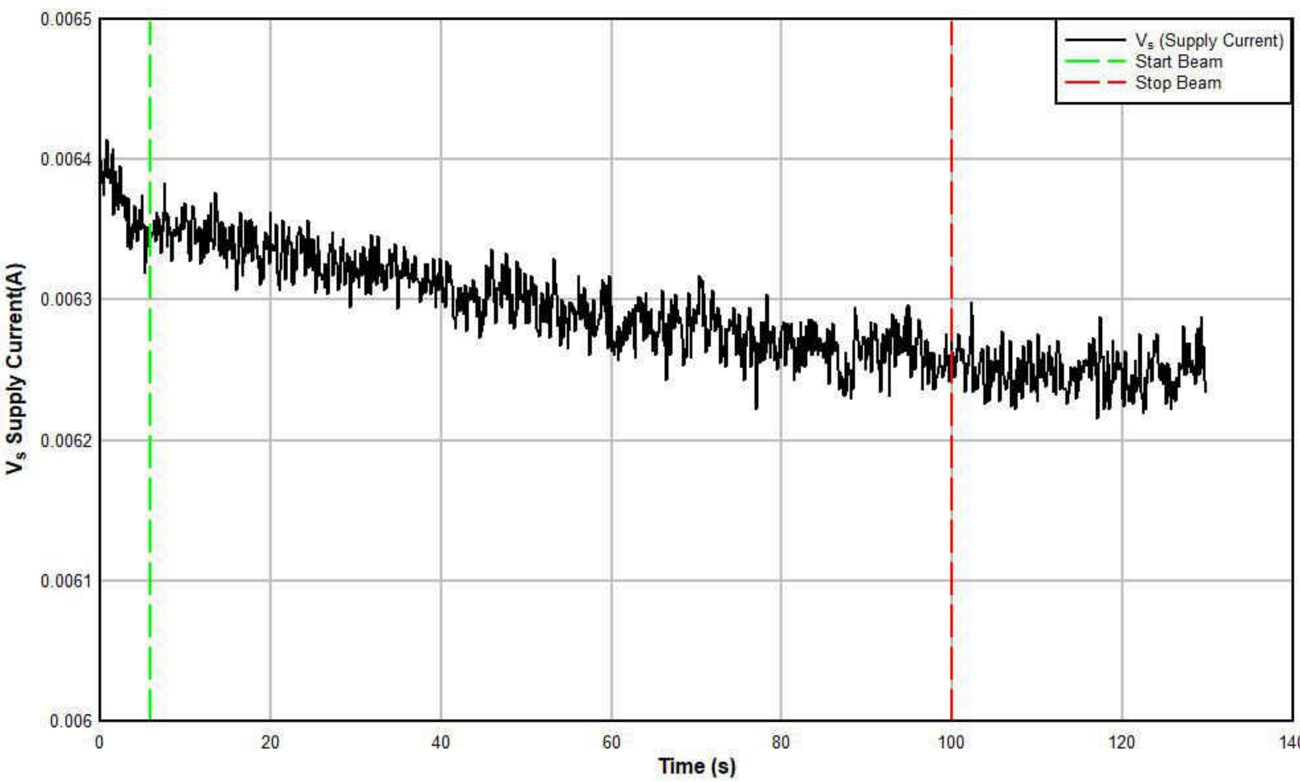

Figure 5-1. Current vs Time (I vs t) Data for V_S Current During SEL Run # 10

6 SET Results

The LMP7704-SP was characterized for SETs from 2 to 85 MeV-cm^2/mg. Table 6-2 lists the ions used for the testing.The device was tested at room temperature in a buffer configuration with the four different setups show in Table 6-1. A flux of 10^4 ions/s-cm^2 was used for all SET runs. The SETs discussed in this report were defined as output voltages that exceeded a window trigger of 5% from the expected output. Both positive and negative upsets were observed during the testing.

Table 6-1. DUT Configurations

Configuration	Gain	Power Supply (±V)	Input (V)	Expected Output (V)	Trigger Window (V)
1	1	1.35	1	1	0.95–1.05
2		6	2	2	1.9–2.1
3	10	1.35	0.1	1	0.95–1.05
4		6	0.2	2	1.9–2.1

Table 6-2. Ions and Incident Angles

LET_{EFF} (MeV-cm^2/mg)	Ion	Angle (Degree)
85	Ho	25.5
75	Ho	0
72	Pr	25.5
65	Pr	0
54	Ag	25.5
48	Ag	0
23	Cu	25.5
9	Ar	0
2	Ne	0

The number of events observed during the heavy ion runs are presented in Table 6-3 to Table 6-6. All four channels were monitored during the heavy ion runs. LMP7704-SP was tested to fluences ranging from 10^6 to 2 × 10^6 ions/cm^2.

Table 6-3. SET Results: V_S = ±1.35 V, Gain = 1

LET_{EFF} (MeV-cm^2/mg)	Fluence (ions/cm^2)	Ch1		Ch2		Ch3		Ch4	
		# of Events	Cross Section (cm^2)	# of Events	Cross Section (cm^2)	# of Events	Cross Section (cm^2)	# of Events	Cross Section (cm^2)
85	9.96E+05	28	2.81E-05	252	2.53E-04	248	2.49E-04	45	4.52E-05
75	1.00E+06	20	2.00E-05	248	2.48E-04	194	1.94E-04	40	4.00E-05
72	1.01E+06	23	2.29E-05	17	1.69E-05	4	3.98E-06	4	3.98E-06
65	9.70E+05	18	1.86E-05	13	1.34E-05	6	6.19E-06	20	2.06E-05
54	2.00E+06	20	1.00E-05	17	8.52E-06	7	3.51E-06	26	1.30E-05
48	1.99E+06	16	8.04E-06	14	7.04E-06	10	5.03E-06	17	8.54E-06
23	2.00E+06	0	0.00E+00	0	0.00E+00	0	0.00E+00	1	4.99E-07
9	1.99E+06	1	5.03E-07	0	0.00E+00	0	0.00E+00	1	5.03E-07
2	2.00E+06	1	5.00E-07	0	0.00E+00	0	0.00E+00	2	1.00E-06

Table 6-4. SET Results: V_S = ±6 V, Gain = 1

LET_{EFF} (MeV-cm²/mg)	Fluence (ions/cm²)	Ch1		Ch2		Ch3		Ch4	
		# of Events	Cross Section (cm²)	# of Events	Cross Section (cm²)	# of Events	Cross Section (cm²)	# of Events	Cross Section (cm²)
85	1.00E+06	14	1.40E-06	67	6.70E-05	41	4.10E-05	28	2.80E-05
75	1.00E+06	16	1.60E-06	53	5.30E-05	59	5.90E-05	11	1.10E-05
72	1.00E+06	14	1.40E-06	15	1.50E-05	10	9.97E-06	13	1.30E-05
65	9.80E+05	13	1.33E-05	11	1.12E-05	20	2.04E-05	12	1.22E-05
54	2.00E+06	21	1.05E-05	17	8.50E-06	16	8.00E-06	18	9.00E-06
48	2.00E+06	21	1.05E-05	24	1.20E-05	10	5.00E-06	18	9.00E-06
23	2.00E+06	2	1.00E-06	0	0.00E+00	0	0.00E+00	6	3.01E-06
9	1.99E+06	0	0.00E+00	0	0.00E+00	0	0.00E+00	0	0.00E+00
2	1.99E+06	0	0.00E+00	0	0.00E+00	0	0.00E+00	0	0.00E+00

Table 6-5. SET Results: V_S = ±1.35 V, Gain = 10

LET_{EFF} (MeV-cm²/mg)	Fluence (ions/cm²)	Ch1		Ch2		Ch3		Ch4	
		# of Events	Cross Section (cm²)	# of Events	Cross Section (cm²)	# of Events	Cross Section (cm²)	# of Events	Cross Section (cm²)
85	1.01E+06	253	2.50E-04	214	2.12E-04	187	1.85E-04	288	2.85E-04
75	9.99E+05	175	1.75E-04	200	2.00E-04	145	1.45E-04	211	2.11E-04
72	9.68E+05	153	1.58E-04	154	1.59E-04	113	1.17E-04	209	2.16E-04
65	1.00E+06	101	1.01E-04	95	9.50E-05	72	7.20E-05	163	1.63E-04
54	2.00E+06	74	3.70E-05	81	4.05E-05	45	2.25E-05	124	6.20E-05
48	2.00E+06	61	3.06E-05	53	2.66E-05	32	1.60E-05	100	5.01E-05
23	2.00E+06	8	4.00E-06	15	7.50E-06	1	5.00E-07	21	1.05E-05
9	1.99E+06	0	0.00E+00	0	0.00E+00	0	0.00E+00	2	1.01E-06
2	1.99E+06	0	00.00E+00	0	0.00E+00	0	0.00E+00	0	0.00E+00

Table 6-6. SET Results: V_S = ±6 V, Gain = 10

LET_{EFF} (MeV-cm²/mg)	Fluence (ions/cm²)	Ch1		Ch2		Ch3		Ch4	
		# of Events	Cross Section (cm²)	# of Events	Cross Section (cm²)	# of Events	Cross Section (cm²)	# of Events	Cross Section (cm²)
85	1.03E+06	22	2.14E-05	32	3.11E-05	20	1.94E-05	38	3.69E-05
75	9.97E+05	27	2.71E-05	20	2.01E-05	27	2.71E-05	34	3.41E-05
72	1.20E+06	22	1.83E-05	19	1.58E-05	24	1.99E-05	35	2.91E-05
65	1.00E+06	19	1.90E-05	14	1.40E-05	27	2.70E-05	30	3.00E-05
54	2.00E+06	31	1.55E-05	19	9.51E-06	38	1.90E-05	65	3.25E-05
48	2.00E+06	27	1.35E-05	19	9.50E-06	21	1.05E-05	27	1.35E-05
23	2.00E+06	2	1.00E-06	0	0.00E+00	1	5.00E-07	2	1.00E-06
9	2.00E+06	0	0.00E+00	0	0.00E+00	0	0.00E+00	2	1.00E-06
2	1.99E+06	0	0.00E+00	0	0.00E+00	0	0.00E+00	0	0.00E+00

Figure 6-1 to Figure 6-8 show the worst-case positive and negative transients at 85 MeV-cm^2/mg for each test configuration. Importantly, no SETs were observed that reached the voltage supply levels.

When testing with V_S = ±1.35 V, Gain = 1, the worst-case positive transient occurred on channel 2 and reached a peak value of 1.189 V. The event lasted 1.2 µs. The worst-case negative transient occurred on channel 1 and reached a peak value of 0.79 V. The event lasted 0.39 µs.

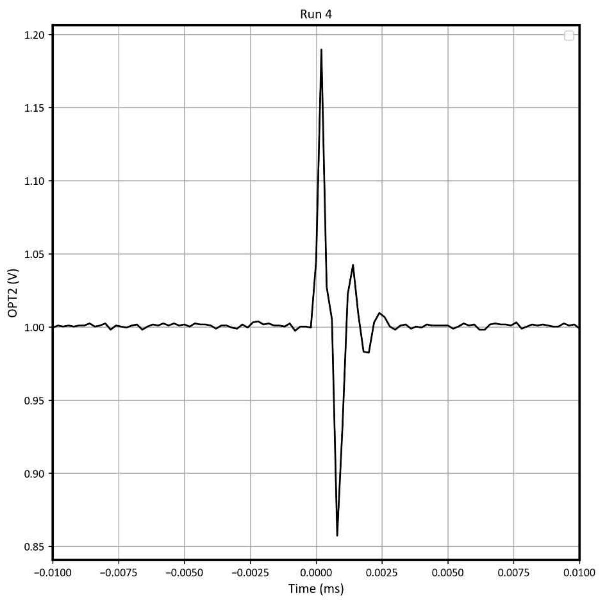

Figure 6-1. Worst-Case Positive Transient on Run #4 With V_S = ±1.35 V, Gain = 1

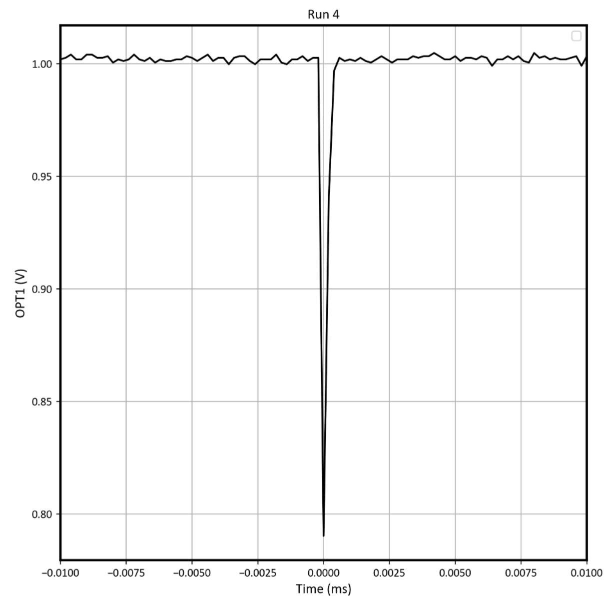

Figure 6-2. Worst-Case Negative Transient on Run #4 With V_S = ±1.35 V, Gain = 1

When testing with V_S = ±6 V, Gain = 1, the worst-case positive transient occurred on channel 2 and reached a peak value of 2.34 V. The event lasted 0.81 µs. The worst-case negative transient occurred on channel 4 and reached a peak value of 1.62 V. The event lasted 0.39 µs.

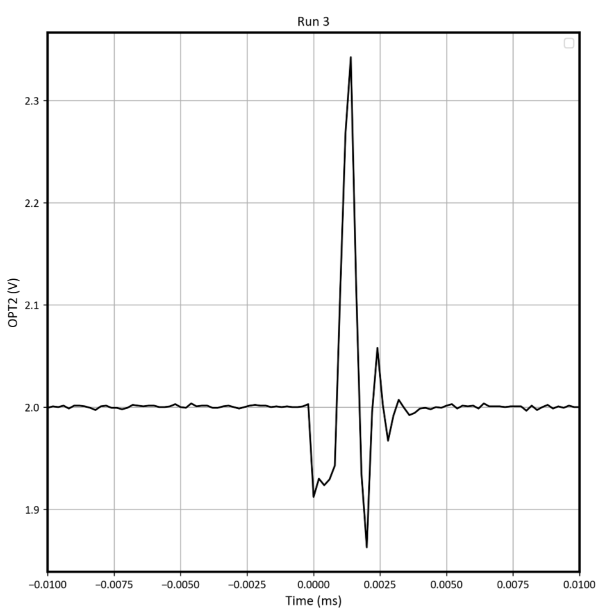

Figure 6-3. Worst-Case Positive Transient on Run #3 With V_S = ±6 V, Gain = 1

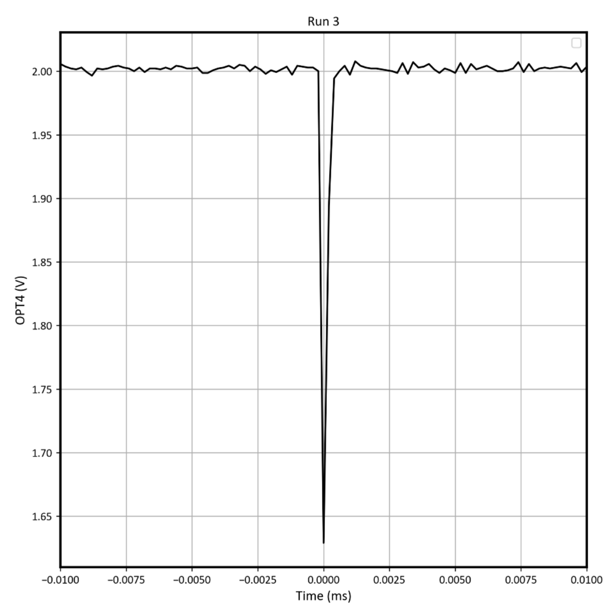

Figure 6-4. Worst-Case Negative Transient on Run #3 With V_S = ±6 V, Gain = 1

When testing with V_S = ±1.35 V, Gain = 10, the worst-case positive transient occurred on channel 3 and reached a peak value of 1.2 V. The event lasted 1.44 µs. The worst-case negative transient occurred on channel 4 and reached a peak value of 0.72 V. The event lasted 1.43 µs.

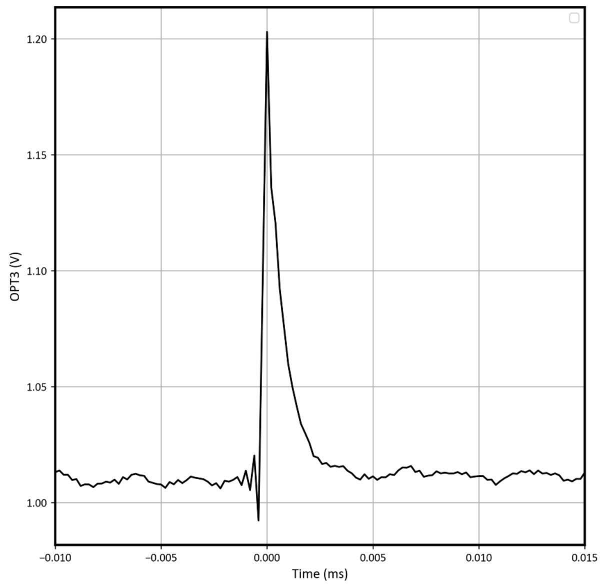

Figure 6-5. Worst-Case Positive Transient on Run #5 With V_S = ±1.35 V, Gain = 10

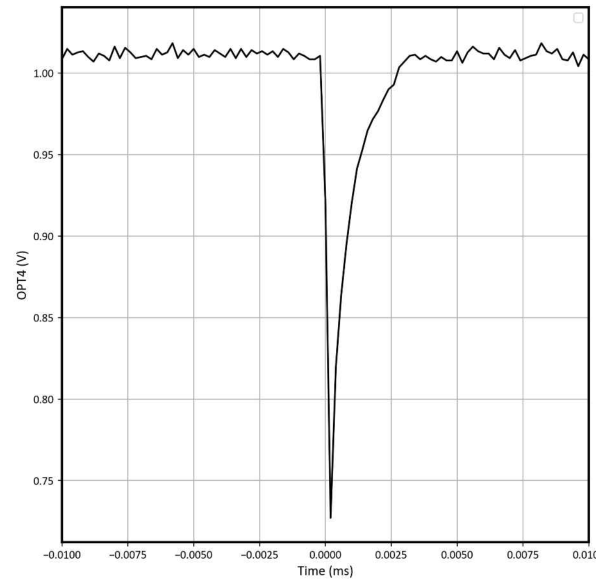

Figure 6-6. Worst-Case Negative Transient on Run #5 With V_S = ±1.35 V, Gain = 10

When testing with V_S = ±6 V, Gain = 10, the worst-case positive transient occurred on channel 4 and reached a peak value of 2.56 V. The event lasted 0.32 µs. The worst-case negative transient occurred on channel 1 and reached a peak value of 1.7 V. The event lasted 2 µs.

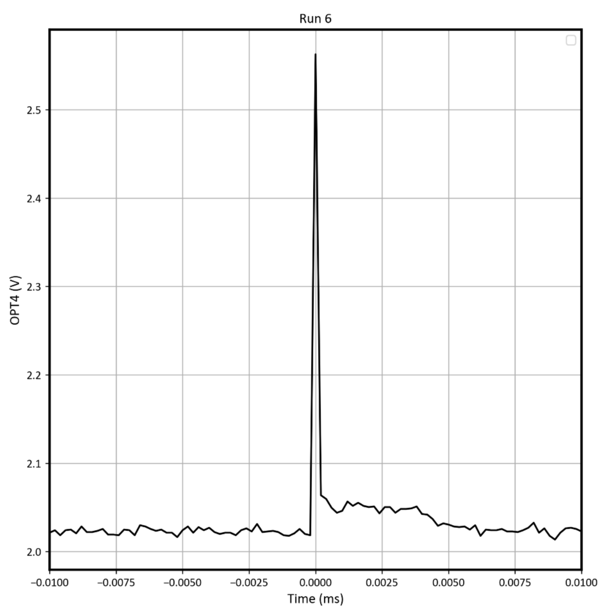

Figure 6-7. Worst-Case Positive Transient on Run #6 With V_S = ±6 V, Gain = 10

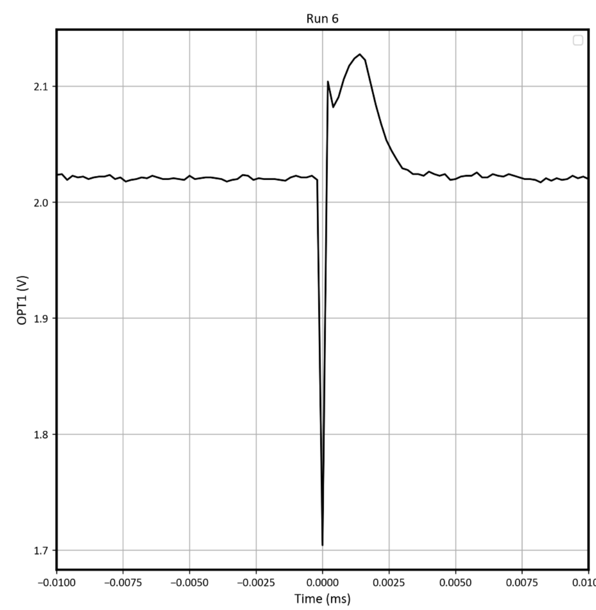

Figure 6-8. Worst-Case Negative Transient on Run #6 With V_S = ±6 V, Gain = 10

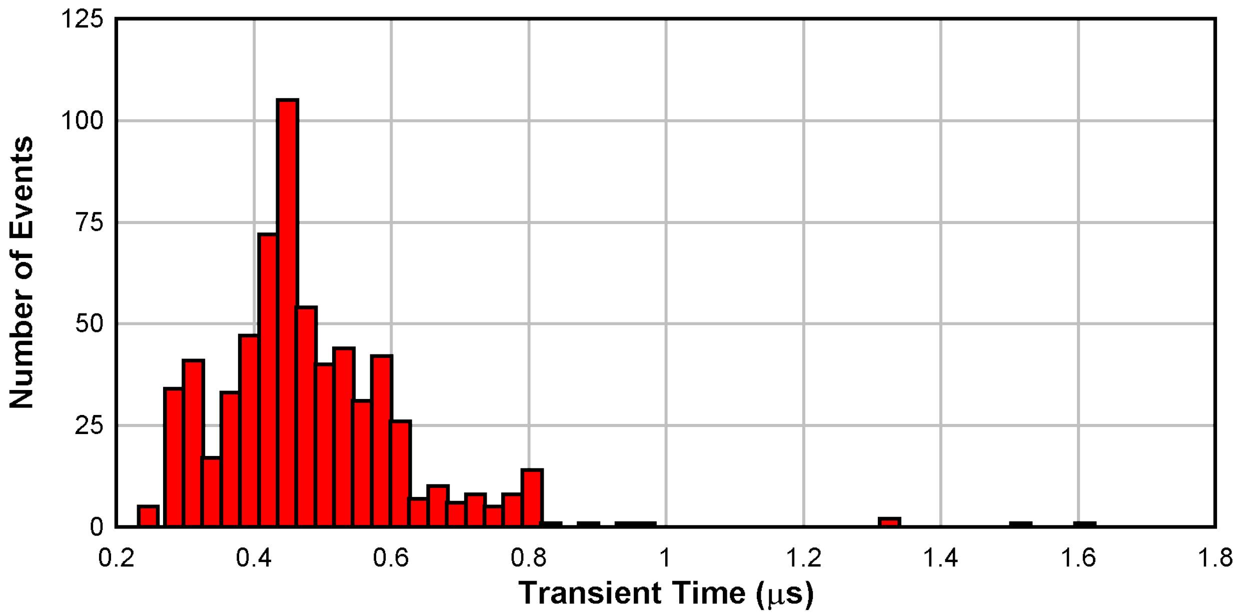

Figure 6-9. Histogram of the Transient Recovery Time for Each Upset at Supply Voltages of ±1.35 V and a Gain of 1

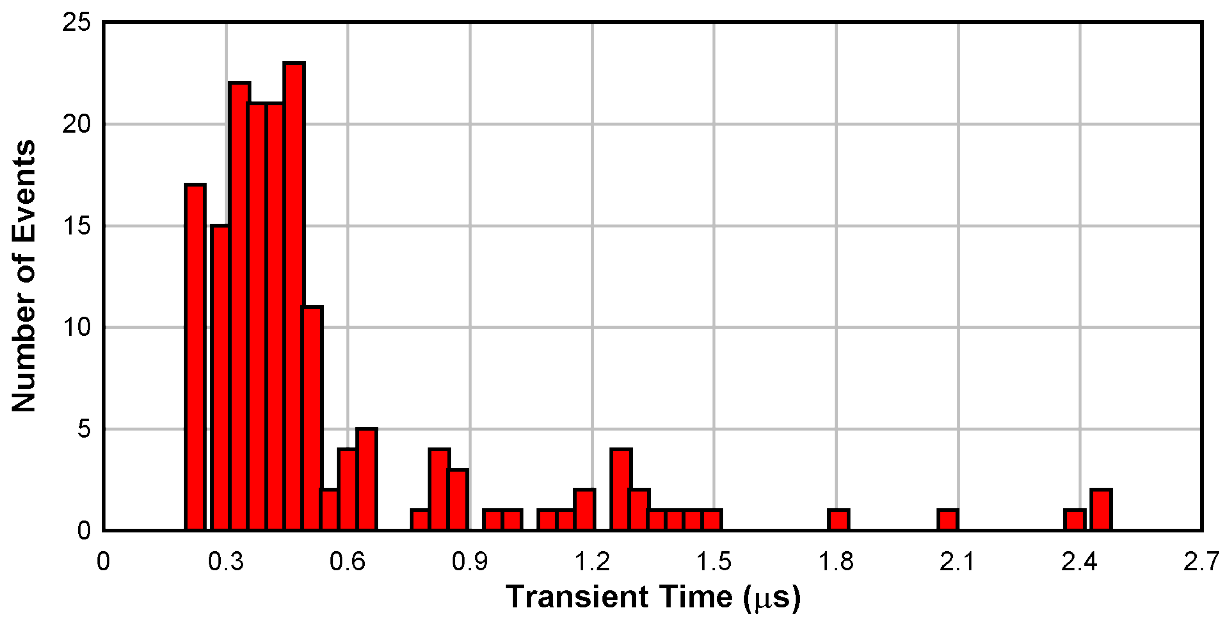

Figure 6-10. Histogram of the Transient Recovery Time for Each Upset at Supply Voltages of ±6 V and a Gain of 1

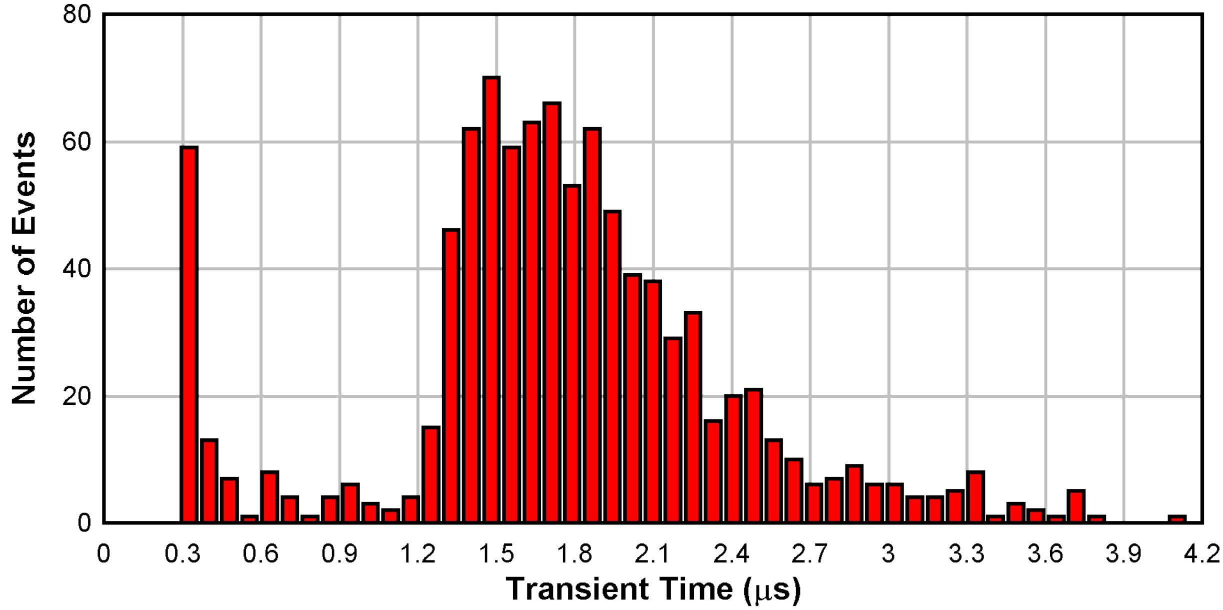

Figure 6-11. Histogram of the Transient Recovery Time for Each Upset at Supply Voltages of ±1.35 V and a Gain of 10

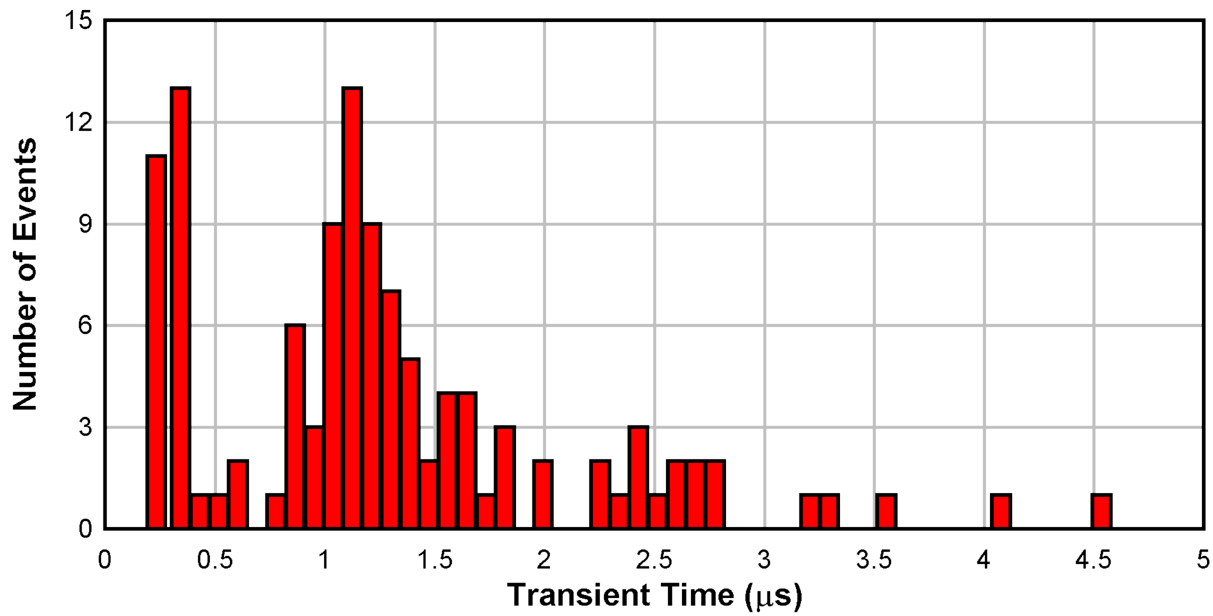

Figure 6-12. Histogram of the Transient Recovery Time for Each Upset at Supply Voltages of ±6 V and a Gain of 10

Figure 6-13 through Figure 6-28 show the plots of the SET cross section versus LET for the different operating modes used during SET testing for each channel. At low LETs, a very low number of transient events (≤ 2) occurred, resulting in different onsets from channel to channel. This causes the cross section plots to look different for each channel.

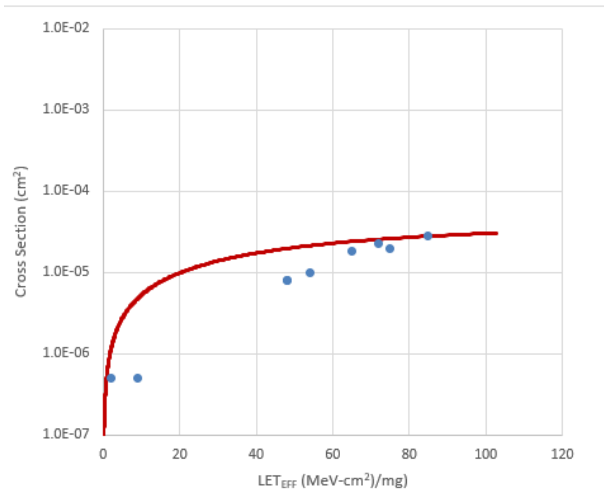

Figure 6-13. Weibull Plot: V_S ±1.35 V and Gain = 1 - Channel 1

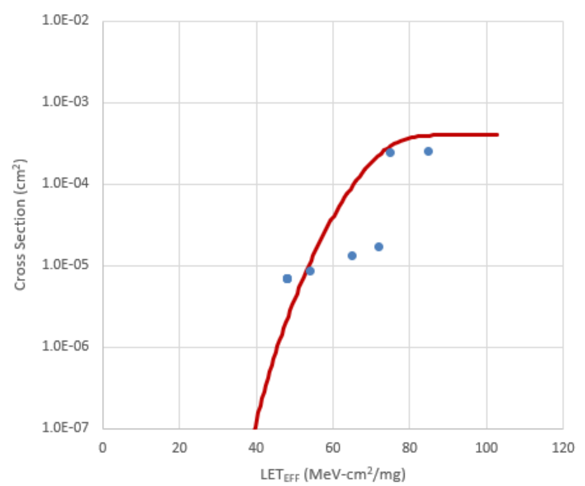

Figure 6-14. Weibull Plot: V_S ±1.35 V and Gain = 1 - Channel 2

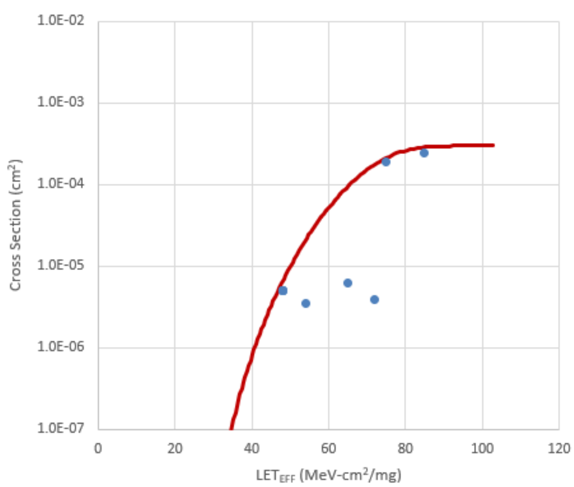

Figure 6-15. Weibull Plot: V_S ±1.35 V and Gain = 1 - Channel 3

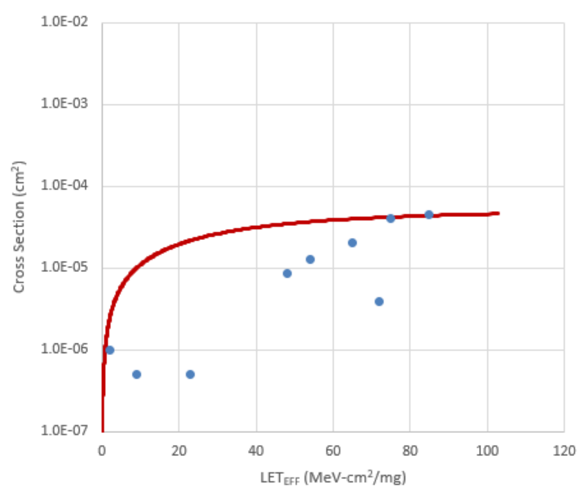

Figure 6-16. Weibull Plot: V_S ±1.35 V and Gain = 1 - Channel 4

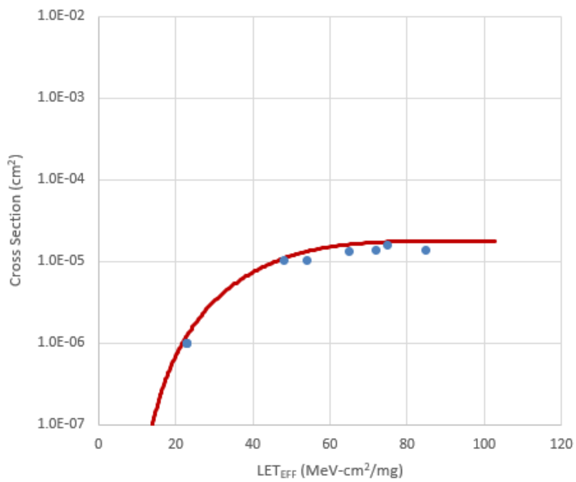

Figure 6-17. Weibull Plot: V_S ±6 V and Gain = 1 - Channel 1

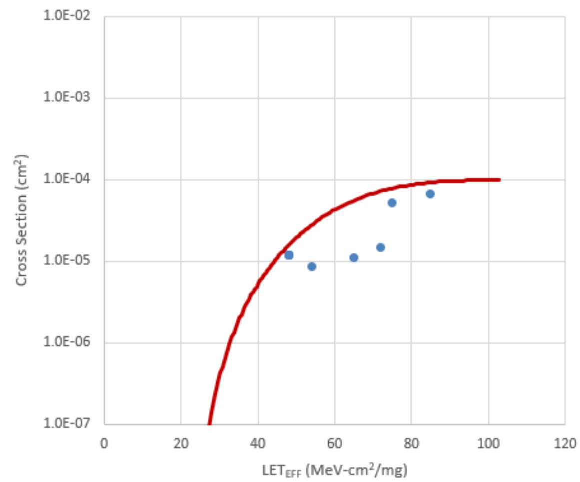

Figure 6-18. Weibull Plot: V_S ±6 V and Gain = 1 - Channel 2

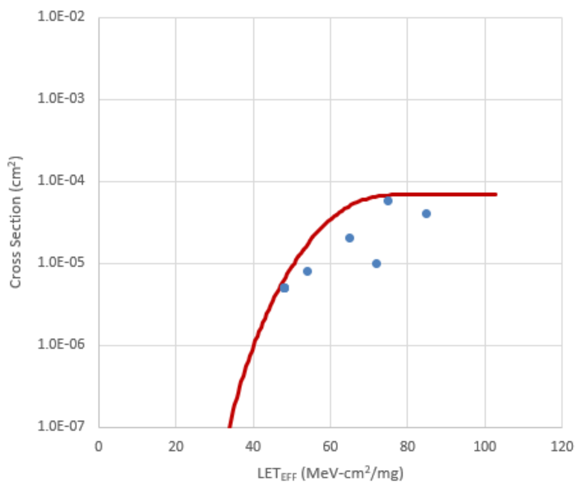

Figure 6-19. Weibull Plot: V_S ±6 V and Gain = 1 - Channel 3

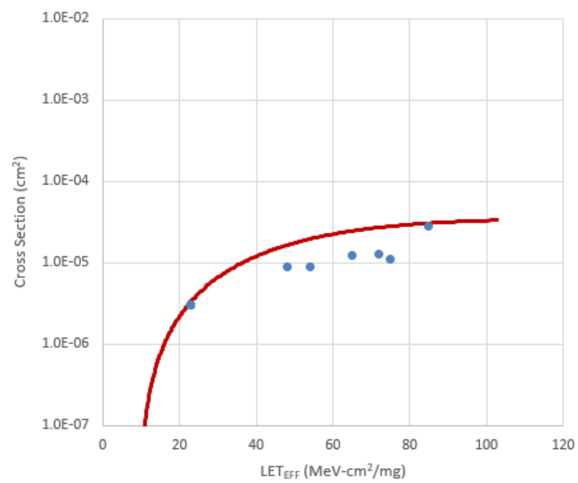

Figure 6-20. Weibull Plot: V_S ±6 V and Gain = 1 - Channel 4

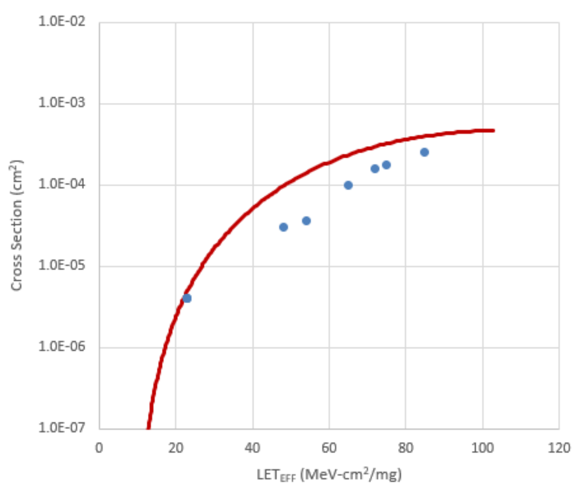

Figure 6-21. Weibull Plot: V_S ±1.35 V and Gain = 10 - Channel 1

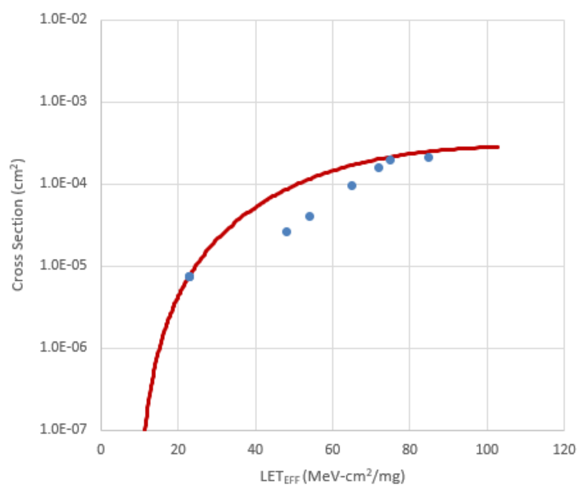

Figure 6-22. Weibull Plot: V_S ±1.35 V and Gain = 10 - Channel 2

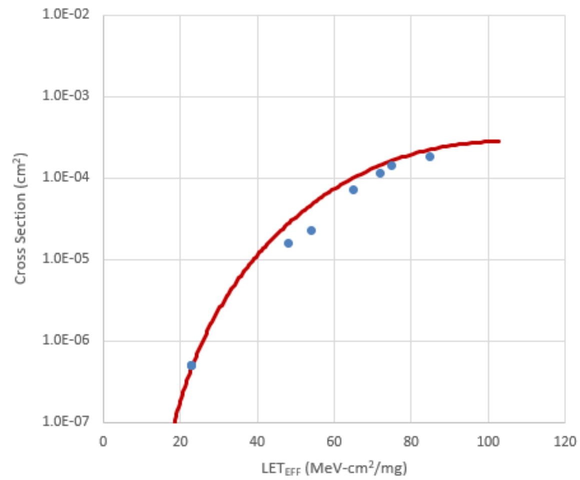

Figure 6-23. Weibull Plot: V_S ±1.35 V and Gain = 10 - Channel 3

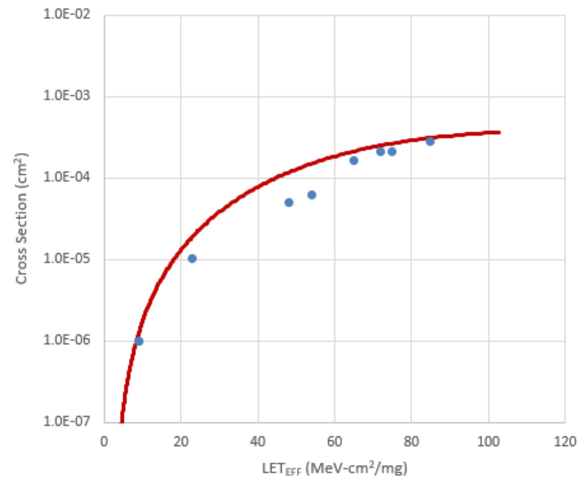

Figure 6-24. Weibull Plot: V_S ±1.35 V and Gain = 10 - Channel 4

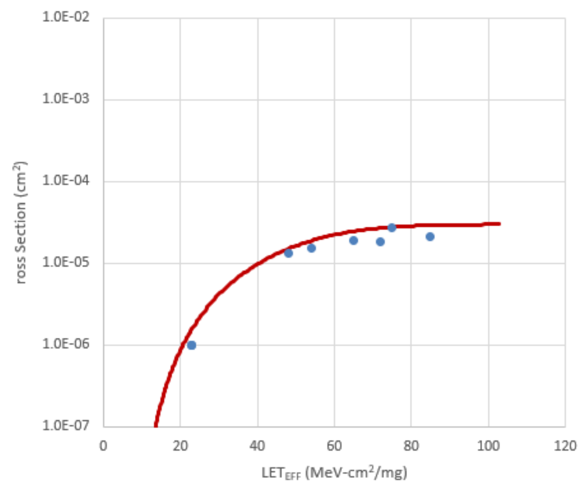

Figure 6-25. Weibull Plot: V_S ±6 V and Gain = 10 - Channel 1

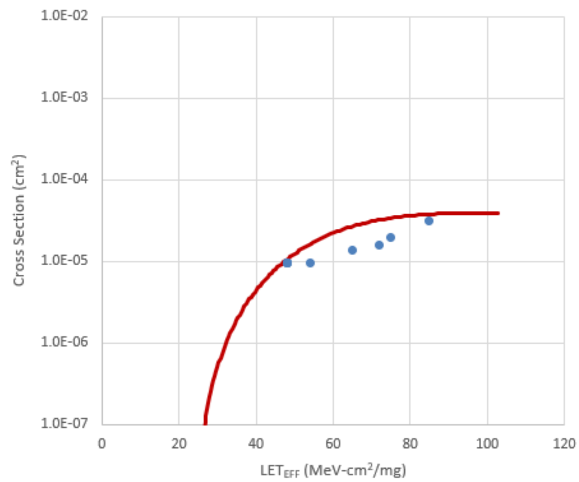

Figure 6-26. Weibull Plot: V_S ±6 V and Gain = 10 - Channel 2

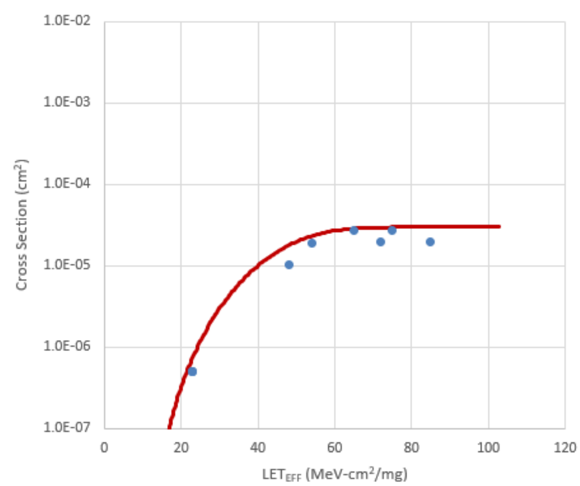

Figure 6-27. Weibull Plot: V_S ±6 V and Gain = 10 - Channel 3

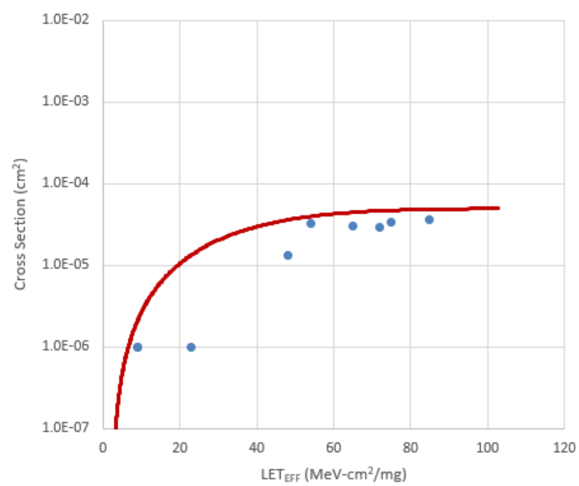

Figure 6-28. Weibull Plot: V_S ±6 V and Gain = 10 - Channel 4

7 Summary

The radiation effects of the LMP7704-SP, a radiation-hardened precision amplifier with a rail-to-rail input and output and CMOS input stage, were studied. This device passed and is latch-up immune up to LET_{EFF} = 85 MeV-cm^2/mg and T = 125°C. SET was characterized from LET_{EFF} = 2 MeV-cm^2/mg to LET_{EFF} = 85 MeV-cm^2/mg. The worst-case transients and the cross-section plots are included. Testing was performed under multiple configurations and supply voltages.

A Confidence Interval Calculations

For conventional products where hundreds of failures are seen during a single exposure, one can determine the average failure rate of parts being tested in a heavy-ion beam as a function of fluence with high degree of certainty and reasonably tight standard deviation, and thus have a good deal of confidence that the calculated cross-section is accurate.

With radiation-hardened parts however, it is difficult to determine the cross-section because often few or no failures are observed during an entire exposure. Determining the cross-section using an average failure rate with standard deviation is no longer a viable option, and the common practice of assuming a single error occurred at the conclusion of a null-result can end up in a greatly underestimated cross-section.

In cases where observed failures are rare or non-existent, the use of confidence intervals and the chi-squared distribution is indicated. The chi-squared distribution is particularly well-suited for the determination of a reliability level when the failures occur at a constant rate. In the case of SEE testing where the ion events are random in time and position within the irradiation area, one expects a failure rate that is independent of time (presuming that parametric shifts induced by the total ionizing dose do not affect the failure rate), and thus the use of chi-squared statistical techniques is valid (because events are rare, an exponential or Poisson distribution is usually used).

In a typical SEE experiment, the device-under-test (DUT) is exposed to a known, fixed fluence (ions/cm^2) while the DUT is monitored for failures. This is analogous to fixed-time reliability testing and, more specifically, time-terminated testing where the reliability test is terminated after a fixed amount of time whether or not a failure has occurred (in the case of SEE tests fluence is substituted for time and hence it is a fixed fluence test). Calculating a confidence interval specifically provides a range of values which is likely to contain the parameter of interest (the actual number of failures/fluence). Confidence intervals are constructed at a specific confidence level. For example, a 95% confidence level implies that if a given number of units were sampled numerous times and a confidence interval estimated for each test, the resulting set of confidence intervals would bracket the true population parameter in about 95% of the cases.

To estimate the cross-section from a null-result (no fails observed for a given fluence) with a confidence interval, we start with the standard reliability determination of lower-bound (minimum) mean-time-to-failure for fixed-time testing (an exponential distribution is assumed) in Equation 2:

$$MTTF = \frac{2nT}{\chi^2_{2(d+1);100\left(1-\frac{\alpha}{2}\right)}} \quad (2)$$

where

- *MTTF* is the minimum (lower-bound) mean-time-to-failure
- *n* is the number of units tested (presuming each unit is tested under identical conditions)
- *T* is the test time
- χ^2 is the chi-square distribution evaluated at 100(1 – α / 2) confidence level
- *d* is the degrees-of-freedom (the number of failures observed)

With slight modification for our purposes we invert the inequality and substitute *F* (fluence) in the place of *T* as shown in Equation 3:

$$MFTF = \frac{2nF}{\chi^2_{2(d+1);100\left(1-\frac{\alpha}{2}\right)}} \quad (3)$$

where

- *MFTF* is mean-fluence-to-failure
- *F* is the test fluence
- X^2 is the chi-square distribution evaluated at 100(1 – α / 2) confidence
- *d* is the degrees-of-freedom (the number of failures observed)

The inverse relation between *MTTF* and failure rate is mirrored with the *MFTF*. Thus the upper-bound cross-section is obtained by inverting the *MFTF* as shown in Equation 4:

$$\sigma = \frac{\chi^2_{2(d+1);\,100\left(1-\frac{\alpha}{2}\right)}}{2nF} \tag{4}$$

Assume that all tests are terminated at a total fluence of 10^6 ions/cm^2. Also assume there are a number of devices with very different performances that are tested under identical conditions. Assume a 95% confidence level (σ = 0.05). Note that as *d* increases from 0 events to 100 events, the actual confidence interval becomes smaller, indicating that the range of values of the true value of the population parameter (in this case the cross-section) is approaching the mean value + 1 standard deviation. This makes sense when one considers that as more events are observed the statistics are improved such that uncertainty in the actual device performance is reduced.

Table A-1. Experimental Example Calculation of MFTF and σ Using a 95% Confidence Interval(1)

Degrees-of-Freedom (d)	2(d + 1)	χ^2 @ 95%	Calculated Cross-Section (cm^2)		
			Upper-Bound @ 95% Confidence	Mean	Average + Standard Deviation
0	2	7.38	3.69E–06	0.00E+00	0.00E+00
1	4	11.14	5.57E–06	1.00E–06	2.00E–06
2	6	14.45	7.22E–06	2.00E–06	3.41E–06
3	8	17.53	8.77E–06	3.00E–06	4.73E–06
4	10	20.48	1.02E–05	4.00E–06	6.00E–06
5	12	23.34	1.17E–05	5.00E–06	7.24E–06
10	22	36.78	1.84E–05	1.00E–05	1.32E–05
50	102	131.84	6.59E–05	5.00E–05	5.71E–05
100	202	243.25	1.22E–04	1.00E–04	1.10E–04

(1) Using a 95% confidence interval for several different observed results (d = 0, 1, 2,…100 observed events during fixed-fluence tests) assuming 10^6 ions/cm^2 for each test. Note that as the number of observed events increases the confidence interval approaches the mean.

B References

1. M. Shoga and D. Binder, "Theory of Single Event Latchup in Complementary Metal-Oxide Semiconductor Integrated Circuits", *IEEE Trans. Nucl. Sci., Vol. 33(6)*, Dec. 1986, pp. 1714-1717.
2. G. Bruguier and J. M. Palau, "Single particle-induced latchup", *IEEE Trans. Nucl. Sci., Vol. 43(2)*, Mar. 1996, pp. 522-532.
3. TAMU Radiation Effects Facility website. http://cyclotron.tamu.edu/ref/
4. "The Stopping and Range of Ions in Matter" (SRIM) software simulation tools website. www.srim.org/index.htm#SRIMMENU
5. D. Kececioglu, “Reliability and Life Testing Handbook”, Vol. 1, PTR Prentice Hall, New Jersey,1993, pp. 186-193.
6. ISDE CRÈME-MC website.https://creme.isde.vanderbilt.edu/CREME-MC
7. A. J. Tylka, J. H. Adams, P. R. Boberg, et al.,"CREME96: A Revision of the Cosmic Ray Effects on Micro-Electronics Code", *IEEE Trans. on Nucl. Sci., Vol. 44(6)*, Dec. 1997, pp. 2150-2160.
8. A. J. Tylka, W. F. Dietrich, and P. R. Boberg, "Probability distributions of high-energy solar-heavy-ion fluxes from IMP-8: 1973-1996", *IEEE Trans. on Nucl. Sci.,Vol. 44(6)*, Dec. 1997, pp. 2140-2149.

C Revision History

NOTE: Page numbers for previous revisions may differ from page numbers in the current version.

Changes from Revision * (February 14, 2023) to Revision A (February 24, 2023) **Page**

- Added clarification of supply voltage conditions to Section 2....................................... 3
- Changed *LMP7704-SP Bias Diagram* in Section 3 to correct V- power supply label....................................... 4
- Changed *LMP7704-SP SEL Conditions* table in Section 5 to correct units for Flux and Fluence....................................... 6
- Changed *SET Results* tables in Section 6 to add units for Fluence....................................... 7

Mailing Address: Texas Instruments, Post Office Box 655303, Dallas, Texas 75265